WWW.IJRPR.COM

International Journal of Research Publication and Reviews

Journal homepage: www.ijrpr.com ISSN 2582-7421

One-Step Morphology and Surface Engineering on 2D Heterostructure toward Superior Dye Adsorption.

Selvan Manigandan[1], Devaraj Nataraj[1,2 *], T.Daniel Thangadurai[3]

[1]Quantum Materials & Devices Laboratory, Department of Physics, Bharathiar University, Coimbatore, Tamil Nadu 641 046, India.
[2]UGC-CPEPA Centre for Advanced Studies in Physics for the Development of Solar Energy Materials and Devices, Department of Physics, Bharathiar University, Coimbatore, Tamil Nadu, India 641 046
[3]KPR Institute of Engineering and Technology, Coimbatore, Tamil Nadu, India 641 407.
*Corresponding author: E-Mail: de.natraj2011@gmail.com

ABSTRACT:

This study demonstrates the fast and efficient removal of organic dye from wastewater using MoS_2/Graphene heterostructure as an adsorbent. The MoS_2/Graphene heterostructure, synthesised via a one-step hydrothermal method, demonstrates excellent adsorption capacity for rhodamine B (RhB) and methylene blue (MB). This is ascribed to 3D morphology self-assembled with two-dimensional sheets, its high specific surface area, and micro nanopores, which provide numerous adsorption sites and uniform coverage for dye molecules. High adsorption efficiency is obtained for RhB (98%) and MB (98.5%) at adsorption equilibrium time for 100 mg/L solution concentration. The faster and more efficient adsorption ensures that MoS_2/Graphene heterostructure is a broad-spectrum adsorbent for different dye contaminants in water.

Keywords: Graphene, MoS_2, Heterostructure, Dye adsorption, Faster removal

1. Introduction

Environmental pollution has recently become the most significant issue of concern. It is getting severe attention due to its harmful and adverse effects on human health and aquatic and other ecosystems worldwide [1]. Industrial wastes have many toxic and dangerous chemicals, including organic dyes from textile industries, printing, leather companies, distillery, electroplating, medicines, and food industries, that significantly threaten natural resources. Most dyes and chemicals are highly water soluble and toxic, which can cause severe damage to the environment and human beings [2]. A significant risk has been falling on water bodies like lakes, ponds, rivers, oceans, etc., leading to a scarcity of clean and fresh water. The industrial discharge of organic dyes into water resources shows several problems as they are part of the ecosystem. Most toxic dyes exhibit carcinogenic, mutagenic, and teratogenic properties in humans and animals [3].

Recently, much effort has been made to remove the harmful and hazardous chemicals and dyes from wastewater and industrial effluents before they are discharged into water bodies and onto terrestrial lands [4]. This effort uses several approaches, including chemical oxidation, membrane separation, filtration, electrochemical treatment, photocatalytic or catalytic degradation, adsorption, etc., to reduce the organic dye interaction within the environment [5]. Recently, photocatalytic degradation has gained widespread interest in degrading dyes, but photocatalytic dye degradation may cause secondary pollutants in an aqueous solution during the chemical reaction [6]. Hence, the adsorption of organic dye molecules with the nanomaterial or activated templates is considered an efficient and economical process, which can easily extend to removing organic dyes at a large scale [7]. Various dye adsorbents such as clays, biomass, polymeric and carbonaceous materials, including activated carbon, graphene-based materials, biomass-derived carbons, and other layered materials, have been utilised to remove organic pollutants and dyes [8]. Though activated carbon is widely used as an excellent adsorbent due to its large surface area and high adsorption capacity, its high cost seriously limits its application [9].

Two-dimensional materials and their three-dimensional architectures have gained immense interest as adsorbent materials for efficiently removing organic contaminants, including various dyes, from wastewater [10]. The high removal efficiencies of graphene-based nanomaterials are highly interesting because of their large surface area and fast accessibility of pollutants to the adsorption sites. Mainly, allotropes of carbons such as graphite, graphene, carbon Nanotubes, and fullerenes appear as 3D, 2D, 1D and 0D, demonstrating distinct chemical and physical properties [11]. As a typical interest, graphene oxide and its derivative are considered ideal adsorbents for treating organic dyes, heavy metals and phenolic compounds from the water [12,13]. However, the synthetic methods of graphene oxide require strong acid/oxidant consumption, and its mass production efficiency is low. Various efforts have been made to overcome this by changing their morphology and electronic structure with doping, hetero-structure formation, and hybridisation with other materials. Apart from the electronic effect, dimensionality also plays a considerable role in exploring the properties of the materials [14].

Particularly in dye-absorbing materials, the design and engineering of 2D materials with 3D morphology give excellent performance in activity, stability, and selectivity towards the reaction environment [15]. 2D geometry gives the materials a high exposed surface area, which is more definite by reducing the thickness, eventually facilitating the contact between the adsorbent surface and the adsorbate [16]. Moreover, the internal atoms could be brought to the surface when the thickness is decreased to monolayer. Thus, more active sites would be available for dye adsorption. It is also possible to introduce defects, unsaturated sites, and/or active edges during the formation of ultrathin structures. Under these conditions, the adsorption-desorption energy barrier is sequentially regulated, facilitating ion mobility or mass transport [17]. Furthermore, some materials beyond graphene, e.g., transition metal chalcogenides (TMDC) and layered double hydroxides (LDH), possess improved electronic conductivity at ultrathin features, as in the case of atomic-thickness nanosheets [18].

Molybdenum disulfide (MoS_2) has recently attracted attention in electronics, photonics, and optoelectronics applications. Due to their unique physical, optical and electrical properties, they include hydrogen evolution reaction field-effect transistors and photodetectors [19]. MoS_2 exhibits different crystalline phases, the most stable semiconducting (2H) and metastable (1T) structures [20]. Moreover, MoS_2 can be easily synthesised on a large scale at a low cost, such as in hydrothermal and liquid exfoliation methods. Constructing heterostructures by stacking different layered materials such as MoS_2 and graphene, benefitting primarily from the chemical interactions between components on their interface, these analogous nanostructured materials with enhanced specific surface area become promising building blocks for a diverse range of next-generation nanomaterial architectures [21].

This paper reports on flower-like MoS_2/Graphene heterostructure formation by the single-step hydrothermal process with citric acid as a graphene source. The prepared MoS_2/Graphene heterostructure demonstrates superior dye adsorption (Rhodamine B, Methylene Blue) capacity. Furthermore, a series of dye adsorption experiments evidence that 98.5% of dye molecules are removed from water within 2 min. Interestingly, after being washed with the methanol solution, the MoS_2/Graphene heterostructure recovered its superior adsorption ability, exhibiting its regenerable property.

2. Experimental Methods

Synthesis of MoS_2**/Graphene heterostructure**. The MoS_2/Graphene heterostructure samples were prepared using a one-step hydrothermal method. In a typical experiment, 0.123 g of Hexa ammonium heptamolybdate tetrahydrate ($(NH_4)_6Mo_7O_{24}\cdot 4H_2O$), 0.114 g of Thiourea 0.5g of citric acid were dissolved in 20 mL of deionised water. Then, 0.5 g Citric acid was added to the above solution and stirred for 30 min, followed by ultrasonic dispersion for 1 h. Finally, the solution was transferred to a 40 mL Teflon-lined autoclave, which was kept in an oven at 200 °C for 24 h. After cooling to room temperature, the black precipitate was collected by centrifugation, washed with water and ethanol three times, respectively, and dried in a vacuum at 60 °C for 12 h. The adsorption capacity of the MoS_2/Graphene heterostructure was compared with pure MoS_2, which was synthesised using the above physical conditions without citric acid.

Characterisation. A powder X-ray diffraction (XRD) was conducted to determine the phase of the as-synthesized composites, with Cu Kα radiation operated at 40 kV and 30 mA. The morphologies and microstructures of the composites were characterised by employing a field emission scanning electron microscope (SEM, Hitachi S-4800) and a transmission electron microscope (TEM, ZISSLibra 200). The crystal structure and layer number were determined through RAMAN Spectroscopy (LabRAM-HORIBA). The dye adsorption capacity of the synthesised samples was estimated with UV–vis spectra (Agilent carries 400 spectrophotometers) as a function of time.

Dye Absorption Experiments: An aqueous solution with various dye concentrations of RhB and MB was used as model dyes to examine the adsorption characteristics of the MoS_2/Graphene heterostructure. The adsorption behaviour measurement of dyes was conducted according to the following procedure: 0.02 g of as-prepared MoS_2/Graphene heterostructure was dispersed into 50 mL of RhB solution with different concentrations, that is, 50, 60, 70, 80, 100, 200 mg/L, respectively. Then, the solution was stirred vigorously with a magnetic stirrer. The RhB solutions were taken out at different intervals (10, 20, 30, 60min) and immediately centrifuged at 12000 rpm for 3 min. The concentrations of RhB were analysed at 553 nm with a UV−vis spectrometer. The following equations were used to calculate the adsorption capacity and mechanism:

$$Qt = (C_0 - Ct)\ V/W \quad \text{----------(1)}$$

$$E_r = 100*(C_0 - Ct)\ C_0 \quad \text{----------(2)}$$

Where Qt (mg/g) is the adsorption capacity at different times, C_0 (mg/L) is the initial concentration of the dye solution, Ct (mg/L) is the concentration of the dye solution at time t of adsorption, V (L) is the volume of the dye solution, and W (g) is the weight of the adsorbent. Er is the dye adsorption efficiency [22].

3. Result and discussion

Structural and Morphological Analysis: -

The pure MoS_2 and MoS_2/Graphene heterostructure composite structures were analysed and characterised by XRD to understand the crystalline nature of the as-prepared samples.). Figure 1a shows the XRD pattern of the pure MoS_2 and MoS_2/Graphene heterostructure. All the characteristics peaks of Pure MoS_2 at 2 theta of 14.07^0, 33.41^0, 39.46^0, 50.80^0, and 59.01^0 due to the diffraction from (002), (100), (103),(105),(110) planes, respectively. Further, it can be assigned to the Molybdenite 2H phase MoS_2(JCPDS card number 37-1492) [23]. Subsequently, theMoS_2 /Graphene composite also shows the

ideal MoS_2 X-ray diffraction pattern with peak broadening and shift of 002 planes in its peak position from $14.07^0$to 13.17^0, which results from the interlayer expansion on MoS_2 due to the incorporation of graphene into the MoS_2 lattices [24].

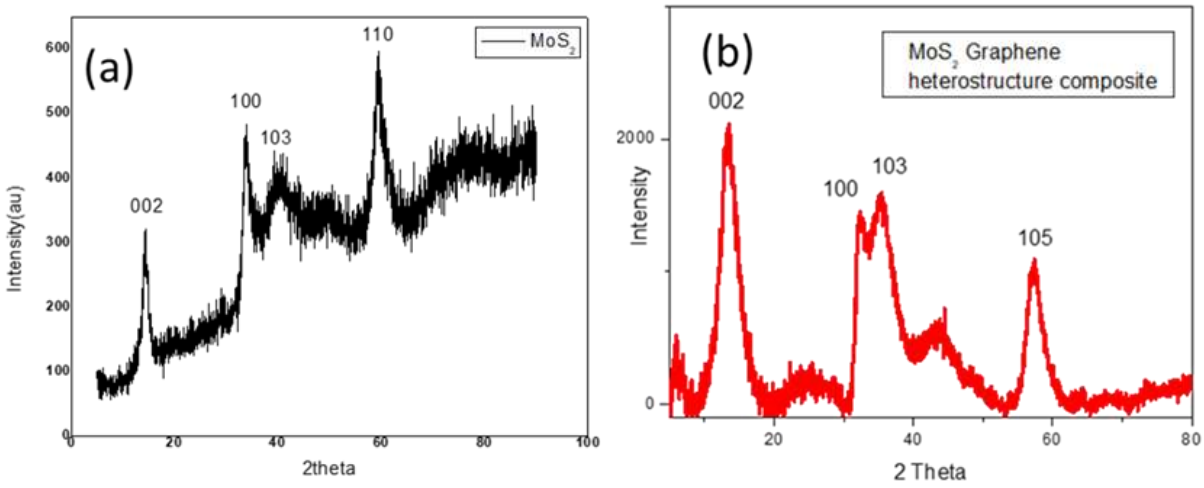

Figure1. Powder XRD patterns of (a) MoS_2 and (b) MoS_2/Graphene heterostructure synthesized through Hydrothermal method

SEM and TEM analysis characterised the morphology of the as-obtained and MoS_2 / Graphene heterostructure composite particles. The representative's mages show that the synthesised particles are flower-like, consisting of several or few Ultra-thin MoS_2/Graphene layers. The average diameter of the flower-like spheres is 1-10 microns. Further, high-resolution TEM images of the MoS_2/ Graphene heterostructure composite particles composed of a few-layer nm thick MoS_2 and graphene layers overlapped. The calculated interplanar distance of the MoS_2 layer is about 0.62 nm and 0.42 for graphene, and it is also well suited to the XRD diffraction pattern of the 002 planes of the MoS_2 layer [25].

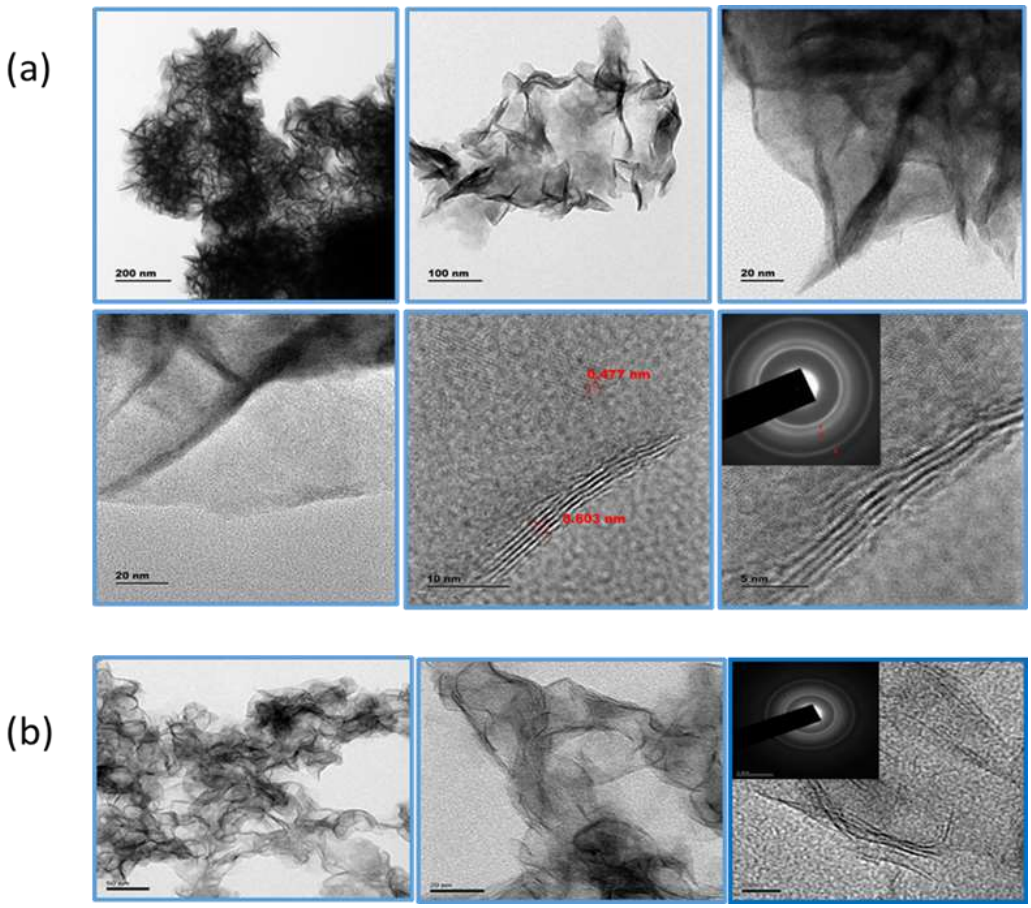

Figure 2. HRTEM images of (a) MoS_2/Graphene heterostructure and (b) MoS_2 synthesized through hydrothermal method

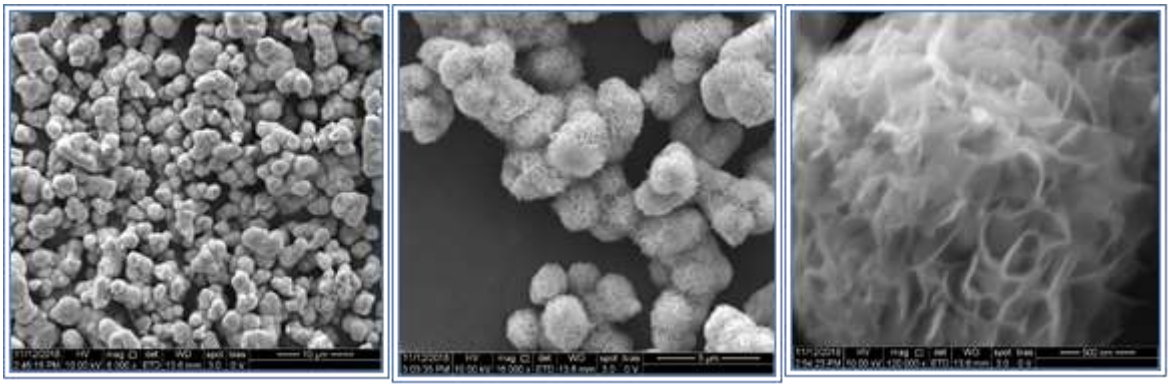

Figure 3. SEM images of MoS_2/Graphene heterostructure

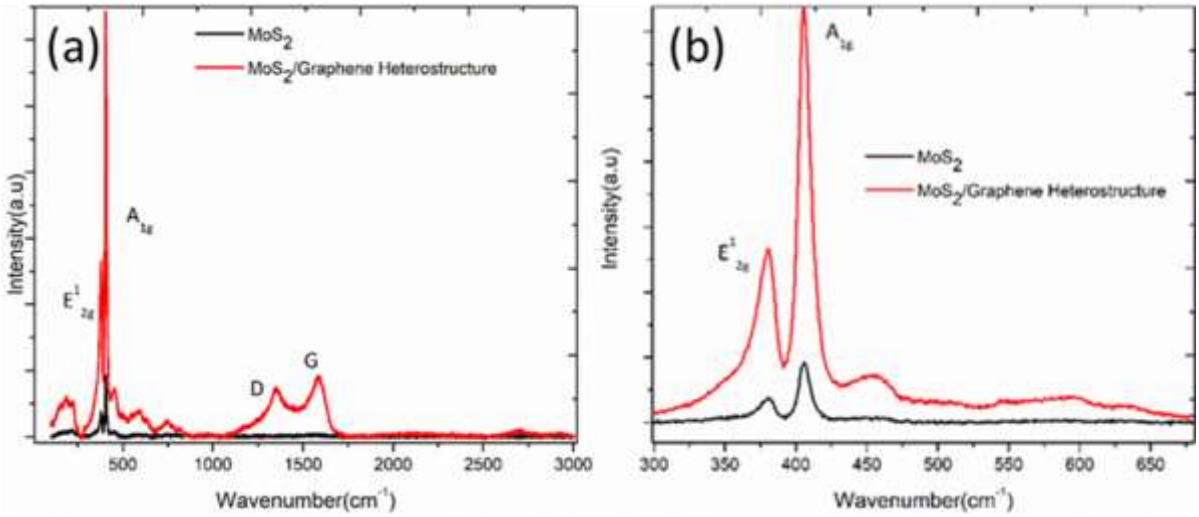

Figure 4. Raman spectra of MoS_2/Graphene heterostructure

Raman spectroscopy is one of the most potent non-destructive tools for studying 2D layered materials, mainly to estimate the crystal structure and number of layers. The crystal lattice of the bulk MoS_2 belongs to the D6h point group symmetry with four Raman active modes. The following irreducible representation represents these zone centre phonon modes: Γ = A1g + 2E2g + E1g, where corresponding Raman bands appear at about 382 and 409 cm−1, assigned to E1 2g and A1g mode, respectively. Figure 4(a), (b) shows the room-temperature Raman spectra of MoS_2 MoS_2/Graphene heterostructure on SiO_2/Si, and as band position matches with bulk MoS_2. The micro-Raman with 532 nm laser is used to understand the crystallinity and chemical composition of the prepared samples. Minimum energy density is used for the study to avoid the oxidation of MoO_3. Raman spectra for MoS_2/Graphene heterostructure were recorded at several places to confirm the structural and composition homogeneity. The two distinct peaks are observed at 382 cm^{-1} and 407 cm^{-1} for the MoS_2 sample, corresponding to the E^1_{2g} and A_{1g} modes, which confirms the formation of the 2H phase MoS_2. The frequency difference between A_{1g} and E^1_{2g} modes is about 25 cm^{-1}, indicating that the formed MoS_2 is multilayer (approx. six layers). In MoS_2/Graphene heterostructure along with E12g and A1g modes, signature Raman modes of graphene D and G are found at 1347 cm-1 and 1584 cm-1, again confirming the successful reduction of citric acid into graphene [26].

Dye absorption measurements:

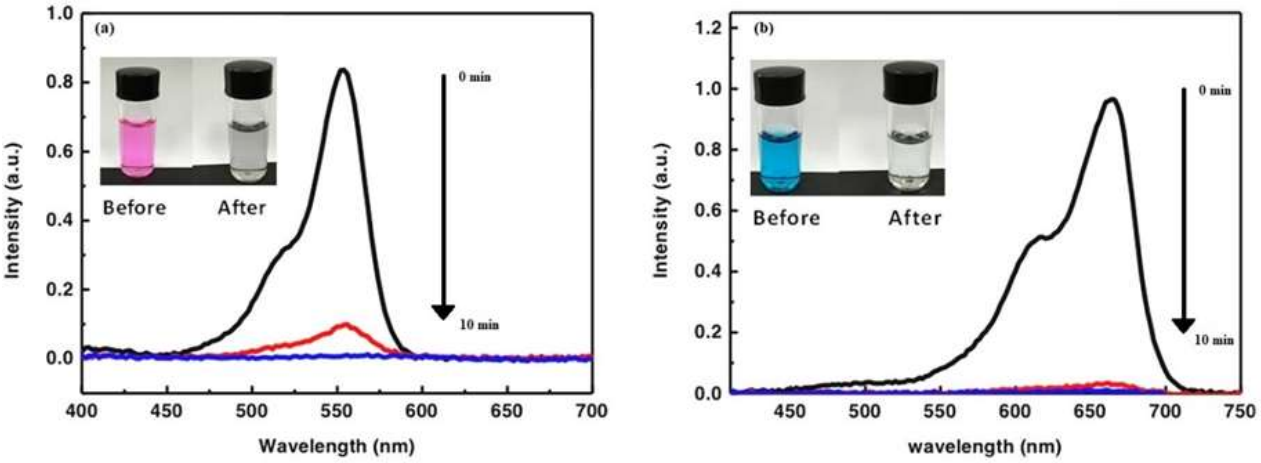

Figure 5. Evolution of UV-vis absorption spectra for (a) RhB (b) MB as a function of time-based on 0.02 g of MoS_2/Graphene heterostructure

As shown in Figure 5, firstly, 0.02 g MoS_2 and MoS_2/Graphene heterostructure were taken to estimate the adsorption capability, and almost 100% dyes (Rhodamine B (RhB) and Methylene Blue (MB)) were removed within 10 min in our experiment. The concentration values of RhB and MB were taken from the absorbance at 550nm, 663nm, and 464nm, respectively. All the experiments were carried out in the dark. Figure 5(a),(b) shows the changes in UV-vis absorption spectra after MoS_2/Graphene heterostructure was added into the dye solution, corresponding to the decrease of dye concentration in the solution. The adsorption process can be divided into two stages in Fig. 5d: the adsorption is very fast due to the high initial dye concentration and unoccupied active adsorption sites at first, followed by a slow stage, and adsorption equilibrium is reached. The adsorption efficiencies for RhB and MB can achieve almost 98% within 30 min. The colour of the solution before and after the MoS_2/Graphene $_{adsorption}$ changed from purple and blue to transparency, indicating the high adsorption capacity of the MoS_2/Graphene heterostructure. To explore the vast adsorption of MoS_2/Graphene heterostructure, the zeta-potential and FTIR were studied to understand the surface property of MoS_2/Graphene heterostructure. Figure 6(b) shows that the obtained MoS_2 has a negative surface charge above pH 3, and the zeta potential increases towards alkaline PH, which indicates the abundant acidic sites on MoS_2/Graphene heterostructure nanosheets. The functional group (-OH, -COOH) may be responsible for the surface negative charge, which is evidenced by the FT-IR spectrum in Fig. 7. Based on the above analysis, electrostatic adsorption could be the main factor in selectively adsorbing positively charged dye such as RhB, MB [27]. The performance of 3D MoS_2/Graphene heterostructure for adsorption of organic dyes from the simulated wastewater using MB and RhB as a representative dye. The interaction between adsorbate and adsorbent is the primary factor that controls the efficiency and selectivity of adsorbent. Nanostructured materials with high adsorption capacity facilitate the reduction of the required quantity of adsorbent and ease the adsorption process. To find the maximum adsorption capacity of the hierarchical MoS_2 /Graphene heterostructure, the adsorption experiments were carried out with 100 mL of an aqueous MB solution, a dye with variable concentrations of 10-200 mg L^{-1}. A 20 mg portion of MoS_2 was used as an adsorbent and added to the dye solution for each concentration. The colour of MB starts to fade away in the presence of MoS_2 nanosheets and suggested the removal of dye from water by adsorption onto the MoS_2 nanosheets. The dye solution samples were drawn as a function of time, and the concentration of MB dye in each sample was examined by measuring their UV−vis absorption spectra. The changes in concentration of MB dye were determined based on absorbance at 663 nm wavelength using a UV−vis spectrophotometer as a function of time. Interestingly, the adsorption of MB on MoS_2 /Graphene heterostructure was found to be very fast at all concentrations ~95% MB dye was adsorbed within 2 min. The physisorption process is believed to be the key driving force for the adsorption of organic dyes. It is a weak adsorption process, and adsorbate is adsorbed onto the surface of the adsorbent by either van der Waals or dipole-driven interaction [27].

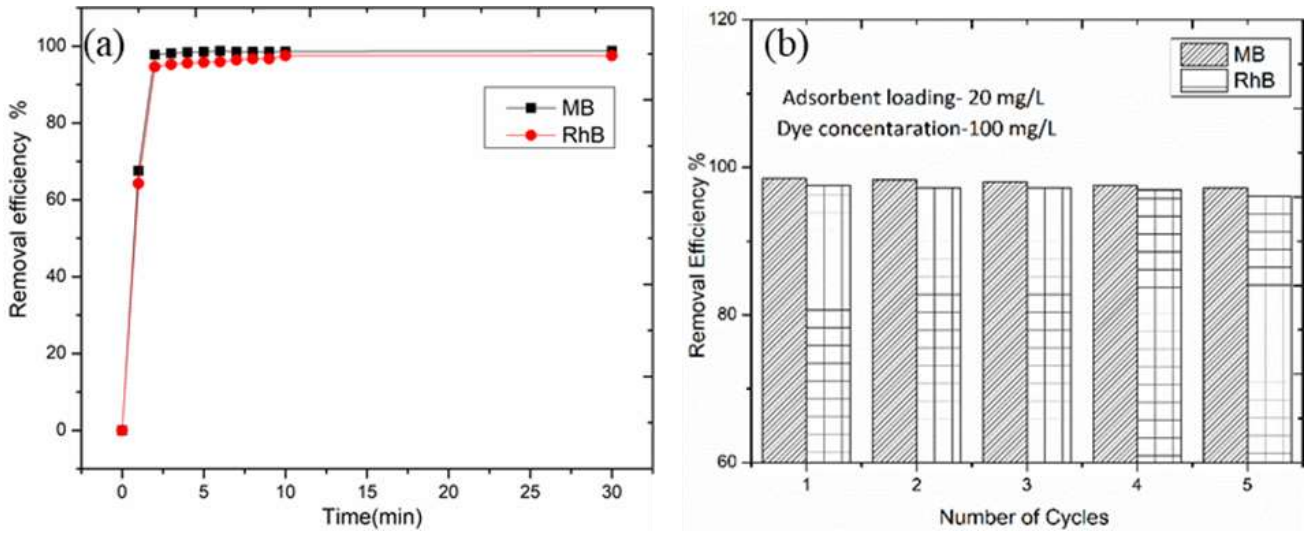

Figure 6. (a) FTIR and (b)zeta potential of MoS2/Graphene heterostructure

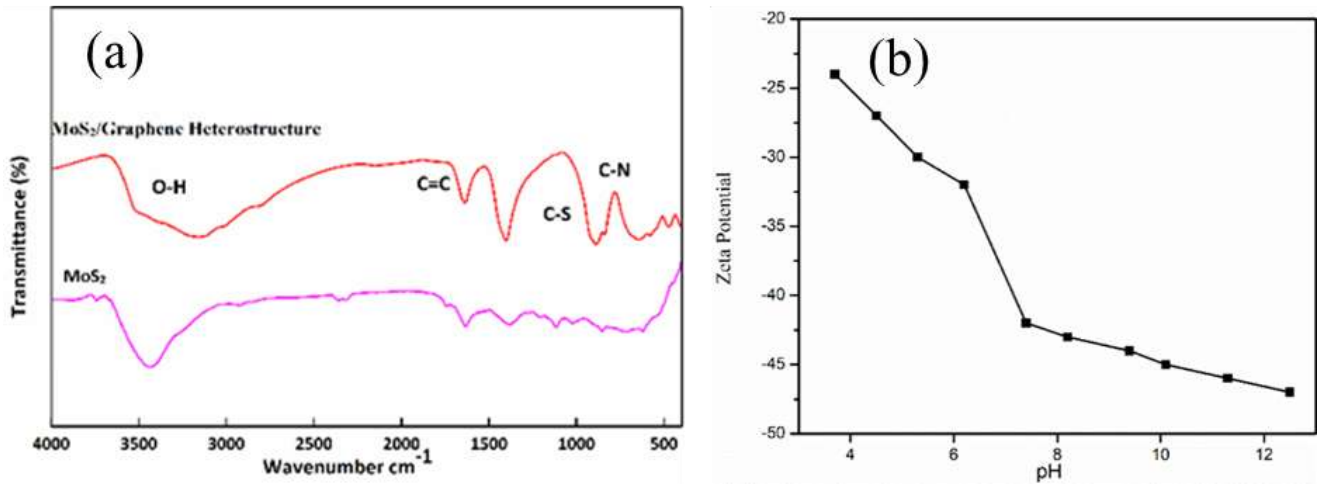

Figure 7. Removal efficiency and re-generality of MoS_2/Graphene heterostructure

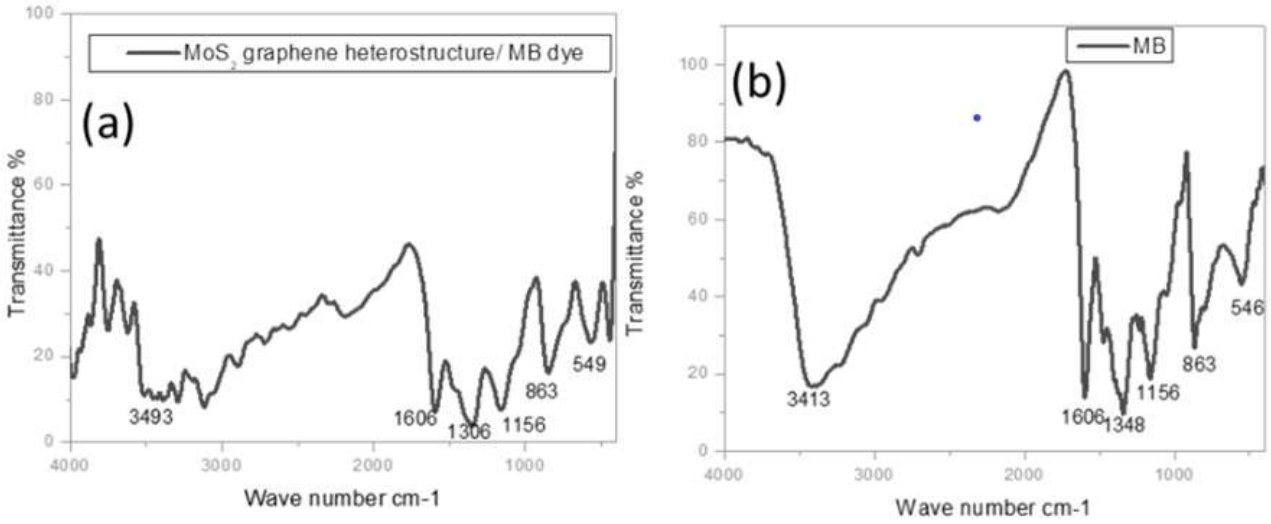

Figure 8. FTIR analysis for the adsorption of MB dye on the surface of MoS_2/Graphene heterostructure.

The MoS_2/Graphene heterostructure collected after the adsorption of MB dye was dried and analysed by FTIR. The FTIR spectrum of MB dye was shown for comparison purposes. The presence of characteristic peaks of MB dye at 1606, 1387, 1348, 1150, 1037, and 863 cm−1 owing to aromatic linkages confirmed the adsorption of MB dye onto the hierarchical microspheres of MoS_2/graphene heterostructure. Moreover, these vibrational modes are not seen in the pristine MoS_2/graphene heterostructure. Furthermore, the Mo−S vibrational mode in recovered MoS_2 after adsorption of MB dye

remains unchanged. Desorption is the process of removal of an adsorbed substance on the adsorbent. The MB RhB dye adsorbed on the MoS_2 was removed using ethanol as an anti-solvent. The residual MoS_2 after desorption of MB dye was recovered and then reused for the subsequent cycle of MB dye adsorption [28].

4. Conclusion

In summary, the flower-like 3D - MoS_2/Graphene heterostructure has been synthesised successfully by a one-step hydrothermal process, which has a superior ability to adsorb various dyes and organic pollutants, especially cationic dyes. The obtained MoS_2/graphene heterostructure samples have negative zeta potential, resulting in superior cationic dye adsorption compared with anodic dye, indicating that the dye adsorption performance depends on its surface charge. The excellent reused ability of MoS_2 has also been confirmed. As a result, the as-synthesized MoS_2/graphene heterostructure is a promising material suitable for high-performance pollutant scavengers for water treatment.

Disclosure of conflict of interest

There is no conflict of interest to be disclosed.

References

[1]. Vorosmarty, C. J; McIntyre, P. B.; Gessner, M. O.; Dudgeon, D.; Prusevich, A.; Green, P.; Glidden, S.; Bunn, S. E.; Sullivan, C. A.; Liermann, C. R.; Davies, P. M. Global Threats to Human Water Security and River Biodiversity. Nature 2010, 467, 555

[2]. Tan, K. B.; Vakili, M.; Hord, B. A.; Poh, P. E.; Abdullah, A. Z.; Salamatinia, B. Adsorption of dyes by nanomaterials: Recent developments and adsorption mechanisms. Sep. Purif. Technol. 2015, 150, 229−242.

[3]. Gupta, V. K.; Suhas. Application of low-cost adsorbents for dye removal - A review. J. Environ. Manage. 2009, 90, 2313−2342.

[4]. Zhao, G.-y.; Liu, L.-j.; Li, J.-r.; Liu, Q. Efficient removal of dye MB: Through the combined action of adsorption and photodegradation from NiFe 2 O 4 /Ag 3 PO 4. J. Alloys Compd. 2016, 664, 169−174.

[5]. Yao, Y.; Xu, F.; Chen, M.; Xu, Z.; Zhu, Z. Adsorption behaviour of methylene blue on carbon nanotubes. Bioresour. Technol. 2010, 101, 3040−3046.

[6]. de Lima, R. O. A.: Bazo, A. P.; Salvadori, D. M. F.; Rech, C. M.; Oliveira, D. D.; Umbuzeiro, G. D. Mutagenic and Carcinogenic Potential of a Textile Azo Dye Processing Plant Effluent That Impacts a Drinking Water Source. Mutat. Res-Gen Tox. En. 2006, 626, 53.

[7]. Wang, Y.; Yao, M.; Chen, Y.; Zuo, Y.; Zhang, X.; Cui, L. General synthesis of magnetic mesoporous FeNi/graphitic carbon nanocomposites and their application for dye adsorption. J. Alloys Compd. 2015, 627, 7−12.

[8]. Luo, P.; Zhao, Y. F.; Zhang, B.; Liu, J. D.; Yang, Y.; Liu, J. F. Study on the adsorption of Neutral Red from aqueous solution onto halloysite nanotubes. Water Res. 2010, 44, 1489−1497.

[9]. Ali, I. New Generation Adsorbents for Water Treatment. Chem. Rev. 2012, 112, 5073

[10]. Ramesha, G. K.; Kumara, A. V.; Muralidhara, H. B.; Sampath, S. Graphene and Graphene Oxide as Effective Adsorbents Towards Anionic and Cationic Dyes. J. Colloid Interface Sci. 2011, 361, 270

[11].Yang, C.; Wu, S. C.; Cheng, J. H.; Chen, Y. C. Indium-based metal-organic framework/graphite oxide composite as an efficient adsorbent in the adsorption of rhodamine B from aqueous solution. J. Alloys Compd. 2016, 687, 804−812.

[12]. Chang, S.-H.; Wang, K.-S.; Li, H.-C.; Wey, M.-Y.; Chou, J.-D. Enhancement of Rhodamine B removal by low-cost fly ash sorption with Fenton pre-oxidation. J. Hazard. Mater. 2009, 172, 1131−1136.

[13]. Zhao, K.; Zhao, G.; Li, P.; Gao, J.; Lv, B.; Li, D. A novel method for photodegradation of high-chroma dye wastewater via electrochemical pre-oxidation. Chemosphere 2010, 80, 410−415. [14]. Jain, R.; Mathur, M.; Sikarwar, S.; Mittal, A. Removal of the hazardous dye rhodamine B through photocatalytic and adsorption treatments. J. Environ. Manage. 2007, 85, 956−964.

[15]. Allegre, C.; Moulin, P.; Maisseu, M.; Charbit, F. Treatment and reuse of reactive dyeing effluents. J. Membr. Sci. 2006, 269, 15−34.

[16]. Bazrafshan, E.; Alipour, M. R.; Mahvi, A. H. Textile wastewater treatment by application of combined chemical coagulation, electrocoagulation, and adsorption processes. Desalin. Water Treat. 2016, 57, 9203−9215.

[17]. Wang, X. H.; Ding, J. J.; Yao, S. W.; Wu, X. X.; Feng, Q. Q.; Wang, Z. H.; Geng, B. Y. High supercapacitor and adsorption behaviors of flower-like MoS2 nanostructures. J. Mater. Chem. A 2014, 2, 15958−15963.

[18]. Aguiar, C. R. L.; Fontana, E.; Valle, J. A. B.; Souza, A. A. U.; Morgado, A. F.; Souza, S. M. A. G. U. Adsorption of Basic Yellow 28 onto chemically-modified activated carbon: Characterization and adsorption mechanisms. Can. J. Chem. Eng. 2016, 94, 947−955.

[19]. Acar, E. T.; Ortaboy, S.; Atun, G. Adsorptive removal of thiazine dyes from aqueous solutions by oil shale and its oil processing residues: Characterization, equilibrium, kinetics and modeling studies. Chem. Eng. J. 2015, 276, 340−348.

[20]. Lee, C. K.; Liu, S. S.; Juang, L. C.; Wang, C. C.; Lin, K. S.; Lyu, M. D. Application of MCM-41 for dyes removal from wastewater. J. Hazard. Mater. 2007, 147, 997−1005.

[21]. Liu, K. P.; Li, H. M.; Wang, Y. M.; Gou, X. J.; Duan, Y. X. Adsorption and removal of rhodamine B from aqueous solution by tannic acid functionalized graphene. Colloids Surf., A 2015, 477, 35− 41.

[22]. Li, Q.; Zhang, N.; Yang, Y.; Wang, G.; Ng, D. H. L. High Efficiency Photocatalysis for Pollutant Degradation with MoS2/C3N4 Heterostructures. Langmuir 2014, 30, 8965.

[23]. Liu, J.; Zhang, L.; Li, N.; Tian, Q.; Zhou, J.; Sun, Y. Synthesis of MoS2/SrTiO3 composite Materials for Enhanced Photocatalytic Activity under UV irradiation. J. Mater. Chem. A 2015, 3, 706.

[24]. Wang, X.; Ding, J.; Yao, S.; Wu, X.; Feng, Q.; Wang, Z.; Geng, B. High Supercapacitor and Adsorption Behaviors of Flower-Like MoS2 Nanostructures. J. Mater. Chem. A 2014, 2, 15958. [25]. Song, H. J.; You, S.; Jia, X. H.; Yang, J. MoS2 Nanosheets Decorated with Magnetic Fe3O4 Nanoparticles and Their Ultrafast Adsorption for Wastewater Treatment. Ceram. Int. 2015, 41, 13896.

[26]. Nam, S.; Parikh, D. V.; Condon, B. D.; Zhao, Q.; Tarver, M. Y. Importance of Poly (ethylene Glycol) Confirmation for the Synthesis of Silver Nanoparticles in Aqueous Solution. J. Nanopart. Res. 2011, 13, 3755.

[27]. Fu, X.; Wu, D.; Zhou, X.; Shi, H.; Hu, Z Solvothermal Synthesis of Molybdenum Disulfide Hollow Spheres Modified by Cyanex 301 in Water-ethanol Medium. J. Nanopart. Res. 2007, 9, 675.